Electrochemical modification of carbon nanotube fibres†

Antonio Dominguez-Alfaro,‡[a] Ngoc Do Quyen Chau,‡[b] Stephen Yan,[c]
Donato Mancino,[a] Sushma Pamulapati,[c] Steven Williams, [c] Lauren W. Taylor,[c]
Oliver S. Dewey,[c] Matteo Pasquali, [c] Maurizio Prato, [a,d,e] Alberto Bianco *[b]
and Alejandro Criado *[f,a]

Covalent modification of the surface of carbon nanotube fibres (CNTFs) through electrochemical reduction of *para*-substituted phenyldiazonium salts and electrochemical oxidation of an aliphatic diamine is described. Following these strategies, diverse surface functionalities have been introduced while preserving the fibre bulk properties. The corresponding modified CNTFs were fully characterised by Raman spectroscopy, X-ray photoelectron spectroscopy, energy dispersive X-Ray, scanning electron microscopy and electrochemical impedance spectroscopy, exhibiting different surface properties from those of the unmodified CNTFs.

Introduction

Carbon nanotubes (CNTs) are nanomaterials with outstanding electrical, thermal, chemical, mechanical, and biological properties.[1] However, significant translation of their properties to the macroscale level has been attained only recently.[2–4] The production of CNT-based macrostructures, which preserve many properties of CNTs has improved, overcoming applicability challenges. CNTs have been assembled into continuous films,[5] sponges,[6–10] and fibres,[2,11] yielding macrostructures with remarkable properties.

In particular, carbon nanotube fibres (CNTFs) represent one of the most attractive examples of the evolution from nanomaterial to macroscopic structures. Four main routes of preparation were developed in the early 2000s and improved since then: colloidal spinning,[12] direct spinning from chemical vapor deposition (CVD) reactors,[13] dry assembly from CVD-grown CNT carpets,[14] and wet spinning from liquid crystalline solutions of CNTs.[15,16] The latter method yields fibres of neat CNTs with the best combination of mechanical, thermal, and electrical properties. A recent example of their application is their use as the main component in flexible optoelectronic devices for the emerging field of textile electronics.[17] In addition to this set of properties, CNTFs exhibit promising biocompatibility, which allows their employment as suture materials to restore myocardial conduction across epicardial scar.[18] The combined properties of these fibres, together with their scalable production, make them an interesting substrate for the introduction of new surface functionalities, an area that has not been explored so far. However, functionalising individual CNTs alters their processability and electrical and mechanical properties, sometimes compromising their final application.[19,20] To this end, the development of chemical strategies for surface functionalisation of fibres have great potential when preserving the inner CNTF structure unaltered. Thus functional groups are incorporated on the fibre surface for specific properties and applications, such as sensing or targeting.[21] It is well-known that CNTs can be functionalised by different strategies to tailor their properties or enhance the interaction with active species.[22–25] Particularly, diazonium salt reactions represent a versatile method to modify CNTs with different functionalities because of the large number of possible substituents in the phenyl ring. In addition, this chemical modification allows a high degree of functionalisation due to the high reactivity of corresponding phenyl radicals. This radical addition occurs when the decomposition of

[a]*Center for Cooperative Research in Biomaterials (CIC biomaGUNE), Basque Research and Technology Alliance (BRTA), Paseo de Miramón 194, 20014 Donostia San Sebastián, Spain*
[b]*CNRS, UPR3572, Immunology, Immunopathology and Therapeutic Chemistry, ISIS, University of Strasbourg, 67000 Strasbourg, France.
E-mail: a.bianco@ibmc-cnrs.unistra.fr*
[c]*Department of Chemical and Biomolecular Engineering, Department of Chemistry, The Smalley-Curl Institute, The Carbon Hub, Rice University, Houston, TX 77005, USA*
[d]*Department of Chemical and Pharmaceutical Sciences, INSTM, unit of Trieste, University of Trieste, Via L. Giorgieri 1, 34127 Trieste, Italy*
[e]*Ikerbasque, Basque Foundation for Science, 48013 Bilbao, Spain*
[f]*Universidade da Coruña, Centro de Investigacións Científicas Avanzadas (CICA), Rúa As Carballeiras, 15071 A Coruña, Spain. E-mail: a.criado@udc.es*
†Electronic supplementary information (ESI) available. See DOI: https://doi.org/10.1039/d1nr07495d
‡These authors contributed equally to this work.

aryldiazonium salts generate a reactive aryl radical. This decomposition can be carried out thermally or electrochemically. After the radical generation, the aryl structure tends to graft onto substrates that possess high charge density, such as conductive or semiconductive materials. Indeed, this methodology is also widely used, *via* electrografting, on many different substrates, including nanostructures such as single-walled carbon nanotubes (SWCNTs),[26] graphene,[27] and transition metal dichalcogenides,[28] as well as macrostructures such as glassy carbon,[29] carbon fibres,[30] and others.[31,32]

Here, we report the functionalisation of the CNTF surface with different *para*-substituted phenyl groups *via* electrochemical reduction of the corresponding aryldiazonium salts. In addition, we introduce amino groups through the electrochemical oxidation of an aliphatic amine. We demonstrate that well-known electrochemical methods can be extended easily to a novel type of substrate as solution-spun CNTFs, introducing surface functionalities while preserving the fibre bulk properties.

Experimental section

Preparation of the modified electrodes with CNTFs

CNTFs were spun in long lengths (hundreds of meters)[4,11] and were cut in single fibres of 4 cm and connected to a single electronic pin. The fibre surface was modified using two different approaches: the first was a common protocol of electrochemical reduction of aryl diazonium salt, and the second was an electrochemical oxidation of aliphatic amine.[33]

The electrochemical reactions took place in a three-electrode cell, in which CNTFs were placed as working electrode, carbon fibre as counter electrode and Ag/AgCl as reference electrode. Cyclic voltammetry (CV) at 100 mV s^{-1} scan rate was carried out from −0.7 to 0.3 V in the case of the electrochemical reduction experiment and from 0 to 2 V in the case of the electrochemical oxidation. In both cases, TBAPF$_6$ (0.1 M) was used as supported electrolyte in 40 mL of anhydrous acetonitrile (ACN).

General procedure for the reductive electrochemical functionalisation of CNTFs. A 1 cm length CNTF, as working electrode, was immersed in ACN (40 mL), using TBAPF$_6$ as supporting electrolyte. The system was assembled in a three-electrode cell using Ag/AgCl as reference electrode and carbon fibre as counter electrode. Before carrying out the reaction, the electrolytic solutions were deoxygenated by nitrogen bubbling for 15 min. Then, three CV scans were carried out from 0 V to −1 V to condition the fibre. Subsequently, 5 mM of the selected diazonium salt was added to the system and stirred until homogenisation. Electrochemical modification of the fibre was performed through 5 scans from 0.3 V to −0.7 V at a scan rate of 100 mV s^{-1}. After the reaction, the CNTFs were thoroughly washed with ACN and water to remove any adsorbed residual molecule. It should be noted that different reaction conditions (concentration of reagents, scan rate, *etc.*) have been explored (data not shown), obtaining as optimal the

ones mentioned above. A control experiment was performed to elucidate the possible defects created by the potential applied to the fibres. Thus, a reducing potential was applied to the fibre in absence of diazonium salt.

Reduction of the *p*-nitrophenyl functionalised CNTFs. A 1 cm length CNTF previously functionalised with *p*-nitrobenzene diazonium salt was immersed in a solution of PBS (1×) and used as working electrode in a cell having Ag/AgCl reference electrode and carbon fibre as counter electrode. The CV of the cell was recorded three times scanning the potential from 1 V to −1.2 V at a scan rate of 100 mV s^{-1}.

Oxidative electrochemical functionalisation of CNTFs. The system was set up as previously described.[33] After conditioning the fibre by three CV scans from 0 V to 1 V, a solution of 5 mM of ethylene diamine was added. Then, five scans from 0 V to 2 V at a scan rate of 100 mV s^{-1} were performed to oxidise the aliphatic amine. Finally, the fibre was washed with ACN and water and then it was fully characterised. In addition, a control experiment was carried out in absence of the ethylene diamine through three CV scans from 0 to 2 V. The aim of this experiment was to determine the number of defects that do not derive from the proposed chemical modification. The described reaction conditions were obtained after exploring different concentration of reagents, scan rates, *etc.* (data not shown).

Characterisation of CNTF electrodes

The modified CNTFs were characterised by Raman spectroscopy, X-Ray photoelectron spectroscopy (XPS), scanning electron microscopy (SEM), X-ray energy dispersive spectroscopy (EDS), and electrochemical impedance spectroscopy (EIS).

Raman spectroscopy. Raman spectra of CNTFs were acquired using a Renishaw InVia Confocal Raman microscope at different excitation wavelengths: 532, 633, and 785 nm with 1 s of integration time. The selected Raman shift range was from 1000 to 2000 cm^{-1}. Each averaged Raman spectrum presented in this study corresponds to the accumulation of 60 spectra per area, evaluating three different areas (180 points per each analysed sample). As described previously,[2] CNTFs present anisotropic properties derived from CNT alignment. Therefore, in order to acquire accurate Raman measurement, functionalised CNTFs were fixed using tape on a glass substrate oriented 90° from line formed between the fibre and the laser beam (Fig. S2†).[34,35] Accordingly, the Raman spectra show the high quality of the CNTs and therefore the CNTFs observed throughout the low defect content measured along the D band at ∼1325 cm^{-1}. The evaluation of the functionalisation degree of the different functionalisation strategies onto the CNTFs were calculated comparing the intensity ratio of the D band with respect to the G band before and after chemical modification.

X-Ray photoelectron spectroscopy. XPS spectra of CNTF were collected *via* a PHI Quantera XPS microprobe using a monochromated aluminium K$_\alpha$ X-ray source. XPS surveys were performed at a pass energy of 140 eV while high resolution scans were taken at a pass energy of 30 eV for 20–40 sweeps.

Scanning electron microscope and X-ray energy dispersive spectroscopy. The morphology of the CNTF surfaces were characterised by SEM. The CNTFs were cut into short lengths, placed on an aluminium holder with double-sided carbon tape and evaluated at different magnifications. SEM images with elemental identification of the CNTFs were acquired using a field-emission scanning electron microscope (FEI Quanta 400 ESEM FEG) equipped with an energy dispersive X-ray EDS detector. Cross-sections of CNTFs were prepared using an ion milling system with an Ar-ion beam (IM4000, Hitachi High-Technologies).

Electrochemical impedance spectroscopy. EIS was used to evaluate the non-faradaic behaviour, which is observed in the fibre due to porosity, functional groups grafted in the surface, and the electroactive properties of the material. Functionalised CNTFs were placed within a three-electrode cell. The CNTFs were placed as working electrode, 2 mm diameter carbon fibre was the counter electrode, and Ag/AgCl as reference electrode. The measurement was recorded controlling the fibre length, *i.e.*, 1 cm. As a general procedure, the functionalised CNTFs were covered within a hollow glass fibre leaving only the active length in contact with the electrolyte. They were assembled in the cell using 0.1 M (pH 7.4) PBS as supported electrolyte and solvent. The frequency changes were registered in the range from 0.1 to 100.0 Hz, with a Gamry Reference 3000 potentiostat/galvanostat.

Results and discussion

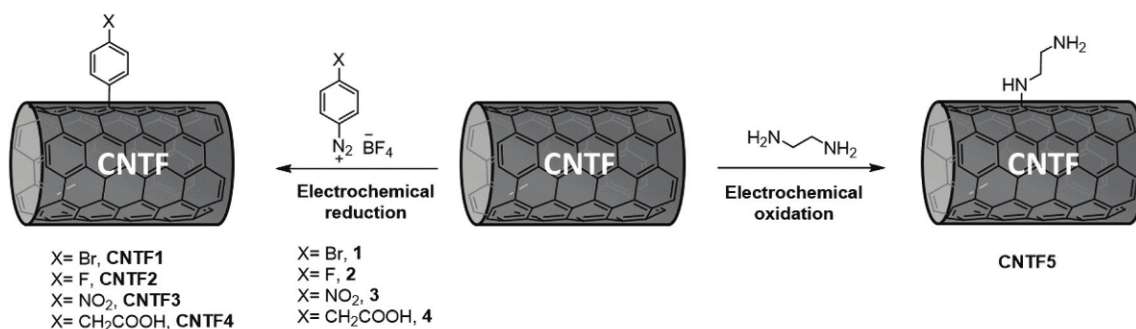## Electrochemical functionalisation of CNTFs

Two different strategies were developed in this work to modify the pristine CNTFs, consisting of an electrochemical reduction of an aryl diazonium salt and an electrochemical oxidation of an aliphatic amine. The general representation of the electrode assembly is shown in Fig. 1. The CNTFs were placed as working electrode, where the reaction takes place under the applied corresponding potential. Then, the modified CNTFs were obtained with different functional organic moieties on their surface.

Thus, five different functional groups were linked to the fibres obtaining: 4-bromophenyl- (CNTF1), 4-fluorophenyl- (CNTF2), 4-nitrophenyl- (CNTF3) and 4-phenylacetic acid-modified CNTF (CNTF4) through electrochemical reduction and ethylene-1,2-diamine-modified CNTF (CNTF5) oxidation (Scheme 1).

Fig. 2 shows the CVs recorded for the CNTF electrodes in the corresponding diazonium salt solutions. The curves exhibit a characteristic irreversible cathodic process that is attributed to the reduction of the diazonium cations present in the reaction medium. When the corresponding aromatic radical is generated, it reacts with the surface of the fibres. The reduction potential values change depending on the substitu-

Fig. 1 Modified CNTFs with *p*-substituted phenyl ring through electrochemical reduction of aryldiazonium salt. Green ball corresponds to a general functional group.

Scheme 1 Electrochemical immobilisation of aryl diazonium salts on the CNTF surface. It is worth noting that chemical representation of CNTFs is depicted as a single carbon nanotube to better illustrate the chemical reactions without reference to the relative sizes of the carbon nanotube and CNTFs.
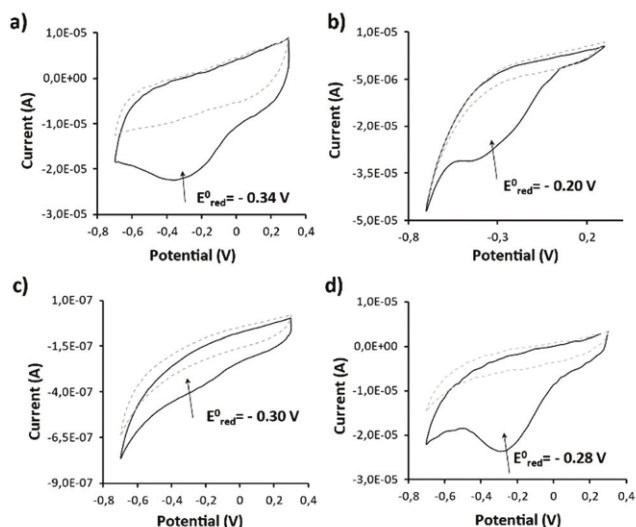
Fig. 2 Cyclic voltammogram corresponding to different diazonium salt reduction using 100 mV s^{-1} as scan rate. First scan (solid line) shows the reduction of the salt, and second scan (dashed line) shows the absence of an active electrochemical surface for further reduction. The panels correspond to the different aryl diazonium salts CNTF1 (a), CNTF2 (b), CNTF3 (c) and CNTF4 (d), respectively.

phitic nanotube structure. As the described electrochemical grafting approach to CNTFs consists of covalently modifying the carbon nanotube surface, therefore Raman spectroscopy was used to verify the functionalisation of CNTFs with the aryl diazonium salts (CNTFs**1–4**) and the ethylene diamine (CNTF**5**).[38] Particularly, the intensity ratio of the D band and the G band (I_D/I_G) values were employed to verify the chemical modification. First, the Raman spectroscopy of pristine (unmodified) CNTFs was investigated using 3 different laser excitation modes (*e.g.*, 532, 633 and 785 nm). In Fig. 3a and Fig. S4,† an average Raman spectrum of ~180 points (from 3 different areas) from the unmodified fibre surface at 532, 633 and 785 nm laser excitation is shown. The G (~1603 cm^{-1}) and G′ bands (~2600 cm^{-1}) indicate the Raman scattering due to strain in the π CNT network. Moreover, the intensity the D band (~1306 cm^{-1}), related to defects and disorders in the graphitic structure, is negligible.

The functionalisation degree of the modified CNTFs derived from diazonium salt CNTFs**1–4** and amine grafting CNTF**5** was compared to pristine material (Fig. 3b). The average I_D/I_G in percentage terms (%I_D/I_G) of the functionalised CNTFs showed a significant difference compared to the

ents of the phenyl ring, corresponding to −0.34 V for CNTF**1**, −0.45 V for CNTF**2**, −0.30 V for CNTF**3** and −0.28 V for CNTF**4**, respectively. Interestingly, the reduction process is complete after the first scan since any additional reduction process is detected in the successive cycles. Presumably, an organic layer around the electrode is formed after the first cycle, blocking the electroactive area that prevents access to new diazonium species.[31,36]
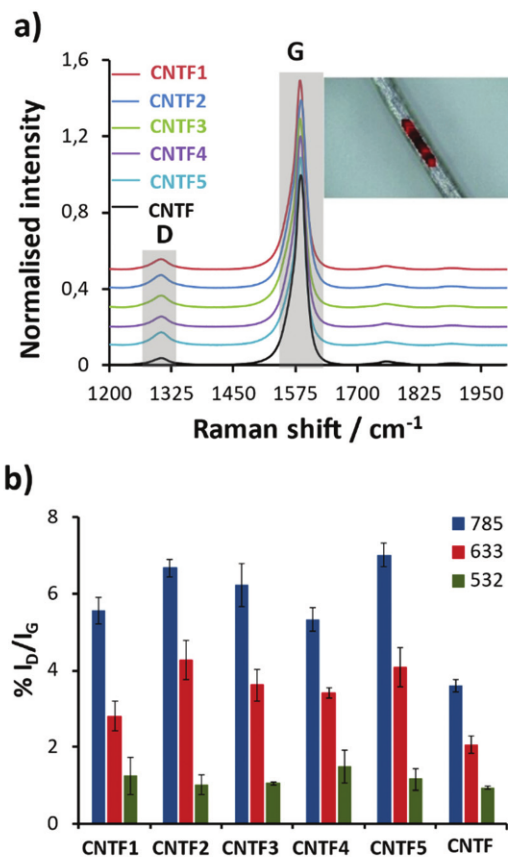
For the electrochemical oxidation approach, the introduction of an aliphatic amine was studied (Scheme 1). As in the previous strategy, the CNTFs were placed as working electrode, using 0.1 M TBAPF$_6$ and 40 mL of ACN. Ethylene diamine was added, and CVs were performed from 0 to 2 V at 100 mV s^{-1}. This oxidative electrografting has been reported for a large number of primary and secondary amines.[31] Previous work has demonstrated oxidation of aliphatic amines carrying out the reaction in aprotic media and using oxidation potentials up to 1 V. A radical cation is generated from one of the removed α proton of the amino group, providing the aminyl species that binds to the surface leading to CNTF**5**.[37] Fig. S3† shows the different voltammograms corresponding to the first and the second scan. A broad peak can be observed in the first scan indicating a chemically irreversible oxidation potential around 1.38 V. This new peak can be attributed to electron oxidation of the amine group that corresponds to the radical cation formation.

Raman spectroscopy characterisation

Raman spectroscopy is one of the most employed and powerful tools for the characterisation of covalent functionalisation of CNTs, since it gives information about additional structural defects disrupting the delocalised electron system in the gra-

Fig. 3 (a) Raman average spectra of pristine CNTFs and functionalised CNTFs at 785 nm from line mapping mode of 180 points analysis, with time exposure of 1 s, and 10% power. Inset: optical image of a typical CNTF with the mapping points analysed (from red to black as intensity colour scale), and (b) %I_D/I_G measured using the different laser sources.

pristine and the control samples (Table S1†). The difference in I_D/I_G ratio with respect to the excitation energy could be related to the metal selectivity of the employed chemical reaction with CNTs.[20] Taking into account that the employed CNTs are a mixture of semiconducting and metallic tubes, in which metallic ones are in higher proportion, the 785 nm laser excitation evidences mainly metallic CNTs, while the 532 nm probes mainly semiconducting in the CNTs used (Fig. S5†). The 633 nm laser excites both CNTs with a higher ratio of semiconducting than metallic. After functionalisation, the change of % I_D/I_G at 785 nm laser excitation is the most prominent with a lower increase for 633 nm excitation, and very little increase for 532 nm. This experimental evidence could be in line with the reported chiral selectivity of diazonium salt reaction towards metallic CNTs.[20] However, it is worth noting that the diameters of CNTs used here are considerably larger than those used by Strano and co-workers, which should make the chiral selectivity of the chemical functionalisation less pronounced.[39] The Raman spectroscopy studies of CNTFs modified through the oxidation of aliphatic amine also suggest metal selectivity. However, further studies are necessary to claim the chiral selectivity since this modification approach for CNTs remains underexplored.

In addition, control experiments were performed on the fibres to clarify the nature of the defects. The electrochemical reduction and oxidation of pristine CNTFs were performed in absence of diazonium salts and diamine, to determine possible defects derived from side-reactions. As shown in Fig. S6,† no significant differences of the %I_D/I_G among the pristine fibre and the control experiments were observed. These results indicate that there are no defects on the surface of the CNTFs due to the reaction conditions.

Therefore, with the enhancement of the percentage of the I_D/I_G ratio of the functionalised fibres in respect to the pristine and control sample values, we can conclude that the electrochemical functionalisation of fibre surfaces with the different *para*-substituted phenyl and amine led to a covalent modification of the external layer of CNTFs.

X-Ray photoelectron spectroscopy characterisation

XPS was then used to identify the type of functional groups on the surface of CNTFs, the chemical state of the atoms, and the relative atomic composition after the electrochemical modifications. The groups introduced through the corresponding phenyl radicals provided a diagnostic signal that allowed to confirm the electrochemical grafting. In particular, the modified CNTF1–3 show the presence of 3.1% of Br, 2.1% of F and 2.6 of N, respectively, while CNTF4 exhibited an increase of 2.7% of O with respect to pristine fibres, and CNTF5 a 3.8% of N (Table S2,† and Fig. S7†). A more detailed identification of the new moieties on the surface of CNTFs is visible in the high-resolution XPS spectra (Fig. 4). The deconvolution of Br 2p signal of CNTF1 displays two peaks at 70.20 and 71.22 eV, corresponding to C–Br bond (Fig. 4a).[40] Likewise, the analysis of F 1s of CNTF2 and N 1s of CNTF3 exhibit peaks at 405.3 and 687.0 eV that can be assigned to C–F and –NO₂ groups,
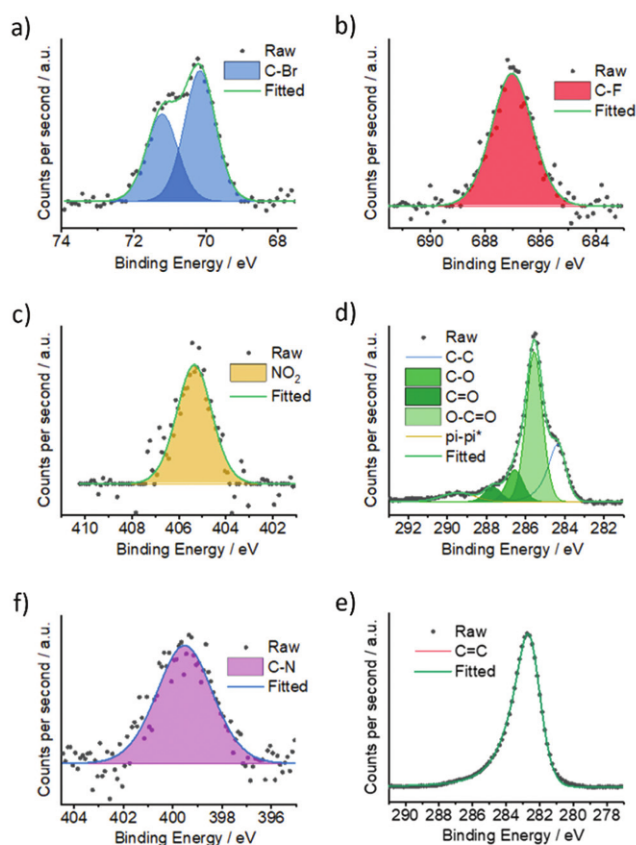
Fig. 4 High resolution XPS spectra of functionalised (a) CNTF1, (b) CNTF2, (c) CNTF3, (d) CNTF4, (e) pristine CNTF, and (f) CNTF5 showing Br 2p, F 1s, N 1s, C 1s, C 1s, N 1s core levels, respectively. It should be noted that the small diameter of CNTFs (~20 μm) makes it difficult to obtain an optimal signal-to-noise ratio.

respectively (Fig. 4b and c). In addition, CNTF4 displays an increment of oxygen content components in C 1s core level after the electrochemical oxidation (Fig. 4d and e). Finally, CNTF5 also presents one peak at 399.5 eV that can be attributed to C–N bond (Fig. 4f). It is worth noting the absence of components at 402–405 eV, therefore, the presence of oxidised nitrogen groups was discarded.[41] However, this fibre, which was functionalised through an electrochemical oxidation, shows C=O and O–C=O groups in the C 1s core level that could be derived from oxidizing side reactions (Fig. S8†).

SEM-EDX characterisation

The morphology of the functionalised fibres was also investigated by SEM. The CNTFs consist of closely-packed and aligned nanotubes with a ~2 nm diameter and CNT length of ~7.4 μm.[42] The functionalisation processes did not significantly alter the physical structure and dimensions of the CNTFs.

EDX analysis, which can provide the elemental composition of the CNTFs, was carried out to know the distribution of the chemical functionalisation on the modified fibres. As representative example, the SEM image along with EDX elemental

maps of CNTF**1** shows a uniform distribution of bromide atoms in the fibre surface (Fig. S9†). The quantitative analysis resulted in an elemental composition of bromide and carbon corresponding to 88.0% and 12.0% (Fig. S10†), respectively. The difference between bromide content for CNTF**1** obtained by SEM-EDX and XPS analysis could be related to the difficulties to select the analysed area in XPS due to its cylindrical shape and low diameter (∼20 μm).

Electrochemical impedance spectroscopy and surface coverage by cyclic voltammetry

EIS is based on small voltage variations in a large window of frequencies, to obtain a specific current with a phase delay. The voltage and current correlation mainly depend on the morphology of the electrodes and the functional groups grafted. Therefore, this correlation observed throughout resistances and capacities, *i.e.*, changes on the relative impedance and phase, can be used to evaluate covalent grafting onto the electrodes, based on variations in the charge transfer ability of the fibre surface.[29,32] In this work, EIS is presented as a tool that confirms the covalent functionalisation evaluated throughout comparative changes in the impedance and phase behaviour.

EIS measurements were performed in a three-electrode cell, where the CNTFs were placed as working electrode, carbon fibre as counter electrode and Ag/AgCl as reference electrode. The measurements were performed in a PBS buffer solution to elucidate how the covalent modifications modulated the original fibre behaviour (Fig. 5 and Fig. S12†).

Since the modified fibres are similar in geometry and composition, and the grafted species do not present redox behaviour, we assume that non-faradaic processes govern the electrode/electrolyte interface, *i.e.*, electrical double layer, ion mobility and chemical surface charges.[43] Fig. 5a illustrates the impedance (modulus) change *versus* the frequency. All CNTFs present the same behaviour, exhibiting a linear dependence with a positive slope at high impedances with low frequencies (1 Hz). Pristine CNTF presents the highest relative impedance (6.31 kΩ) at 1 Hz compared to the phenyl acetic acid CNTF**4** functionalised fibres, which possesses the lowest value (1.81 kΩ) at the same frequency. It is remarkable that the functionalisation of CNTF**4** and CNTF**5**, which possess a charged species (such as p-Ph(CH$_2$COO$^-$) and –(CH$_2$)$_2$–NH$_3^+$) display the lowest values of impedance. However, the fibres with the halogenated heteroatoms (CNTF**1** and CNTF**2**) or an electron withdrawing group (CNTF**3**), which do not have this possibility, showed values of impedance similar to pristine CNTFs, corresponding to 5.79 kΩ and 3.85 kΩ, respectively. The explanation of these results is in line with the description of previous work that reported changes on the local electrical potential due to variations around the electrode of the micro-environmental pH.[43,44] These changes can activate the charge of some species and create strong interactions with the electrolyte, enhancing the transport rates of the cations and the anions inside and outside the pores. Chen *et al.* reported that carboxylic groups attached to SWCNTs can modulate the properties of electrochemical capacitors.[45] The introduction of
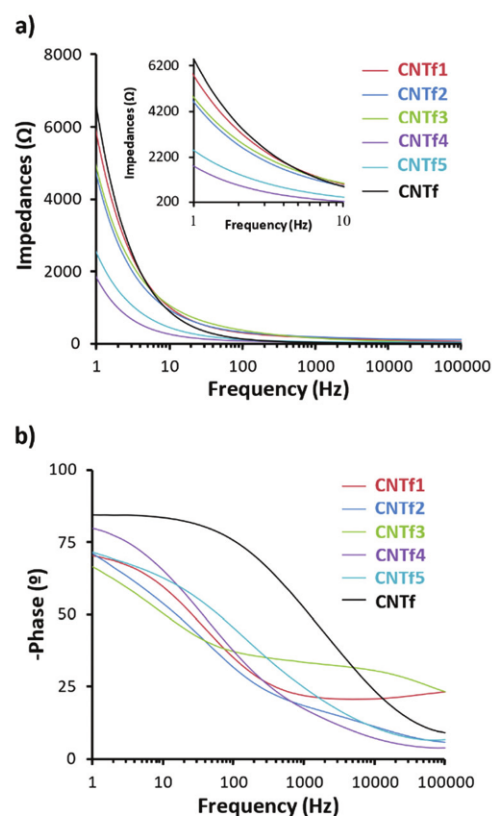
Fig. 5 EIS measurement of (a) relative impedance, inset: expanded area from 1 to 10 Hz, and (b) measurements of functionalised CNTFs in PBS (pH = 7.4, 0.1 M).

carboxylates on electrodes made of SWCNTs can decrease the resistivity of the system and improve the number of sites adsorbed around the SWCNT surface of electrolyte ions, increasing ionic conductivity at electrode–electrolyte interfaces. Charged species such as aliphatic amines also showed a similar behaviour due to micro-changes in the pH closed to the electrode.[43]

Furthermore, Fig. 5b shows the change of phase respect to the frequency. Pristine CNTF phase is −84° at lower frequencies, which is similar to typical values associated with ideal supercapacitors (ϕ = −90°).[46,47] Meanwhile, functionalised fibres present a similar trend, but yield lower values, *i.e.* −80° for CNTF**4**, −66° for CNTF**3** and above −70° for CNTF**1**, CNTF**2** and CNTF**5**. Probably, the reduction of this value of phase on the pristine fibres is due to the formation of lower double layer capacitance than the functionalised fibres. Therefore, this result corroborates the modification of the different CNTFs by significant impedance and phase changes. We would like to evidence that the covalent modification of graphitic structures was previously confirmed by Raman studies,[48] although the physical adsorption of aromatic oligomers typically formed during the diazonium salt decomposition cannot be totally discarded.

An estimation of the modified fibre surface coverage after the grafting reaction can be also obtained *via* electrochemical

characterisation. Taking into account the charge (Q) used during the diazonium salt reduction process, surface coverage (Γ) relates to Q by the following eqn (1):[49]

$$\Gamma = Q/nFA \qquad (1)$$

where n is the number of electrons involved in the process ($n = 1$ in the case of electrochemical reduction of a diazonium salt), F is the Faraday constant, and A is the area of the electrode. Electrode area was calculated as the surface area of a 1 cm long cylinder having a diameter of 25 μm. Q is obtained from the CV of the reduction process, integrating the area under the electrochemical peak, and considering the applied scan rate.

Data obtained with this approach are well-founded in the approximation of a quantitative grafting yield, that is, all the aryl radicals produced by the reduction of the diazonium salt at the working electrode only react to the carbon material to be grafted. By applying eqn (1), the surface coverage on the CNTFs with the different diazonium salts can be calculated (Table 1).

Quantitively, the amount of grafted material on the surface of the fibre ($\Gamma_{reaction}$) results higher than an adsorbed close-packed monolayer of vertically aligned molecules (roughly 12.5 × 10^{-10} mol cm^{-2}).[50] This fact highlights, as we expected, the presence of a thin, homogeneous layer of functionalisation on the outer part of the CNTFs. The higher quantity of functionalisation relative to a monolayer can be explained considering that, as it is often shown by the reaction of diazonium salts, some branching on the functionalisation moiety are formed during the process.[51] This is due to the reaction of reactive radicals not just directly at the surface of the carbon material but also on the aromatic ring of the functionalisation itself. It is worth noting that for simplicity of calculation, we are using the geometrical area of the fibre without regarding to possible roughness of the surface that may increase the actual area *i.e.*, decrease Γ.

To check whether the approximation used reflects what really happens in the electrochemical system, it is necessary to compare the data obtained with eqn (1) from the reduction of the diazonium salt, with a quantitative surface coverage data obtained directly from a functionalised fibre. It was decided to investigate the electrochemical properties of *p*-nitrophenyl functionalised CNTF2. Nitrophenyl groups on the surface of

the fibres are used as redox-labile moieties in a cyclic voltammetry experiment run in 1× PBS solution. Knowing the quantity of charge used in the *p*-nitrophenyl redox processes and using eqn (1), it is possible to get the functionalisation degree of the fibres (Γ_{CNTF3}). It is known that nitrotoluene is reduced in solution to aniline in a 6e$^-$, 6H$^+$ process that also involves the semi-reduced species nitrosotoluene and hydroxylaminotoluene.[52] An example of a CV of a *p*-nitrophenyl functionalised CNTFs from 0.6 V to −1.2 V is shown in Fig. S11.†

In the first cycle, a sharp reduction peak is present at about −1 V, related to the irreversible reduction of NO$_2$ in a multielectron step. This feature completely disappears in the second and following cycles, indicating the full consumption of the moiety during the first sweep. The positive scan of the voltammetry gives rise to a broad peak in between 0 and 0.4 V, generating the associated reduction peak starting from the second scan. This system, according to literature, can be associated to the hydroxylamine/nitroso redox couple in a 2e$^-$ process (Scheme S1†).[53–55]

Remarkably, the system is not fully reduced to the amino compound in the condition in which the CV is run. This may be due to the pH of the electrolyte solution. As expected, the data obtained in this way show a Γ_{CNTF3} (2.37 × 10^{-9} mol cm^{-2}) of CNTF3 lower than the results obtained from the reduction of the diazonium salt 3 (2.91 × 10^{-9} mol cm^{-2}). This result evidence that over the 80% of the radical produced from diazonium salt is grafted to the surface of the electrode. The remaining part is possibly transported in the bulk solution where it quenches.

Conclusions

In summary, we applied fast and versatile electrochemical methods to covalently modified CNTF surfaces. On one hand, by using a simple and widely known electrochemical diazonium reaction, we have covalently attached to the CNTF surface four different *p*-phenyl groups, under easy and mild conditions (reduction potential applied between 0.2–0.4 eV). On the other hand, a covalent modification of CNTFs with an aliphatic diamine was performed by an oxidative electrografting to introduce primary amines in one step.[26] Both chemical modification methods were confirmed by cyclic voltammetry, SEM-EDX, Raman spectroscopy and XPS. In addition, EIS was used to evaluate and confirm the functionalisation onto the fibres. Charged moieties as carboxylic and amines demonstrated lower impedance than *p*-halogenated and *p*-nitro functionalisation at 0.1 Hz. Besides, changes in the phase behaviour confirmed the modification of the fibres with the functional groups and suggested decreasing of double layer capacitance typically observed in this type of carbon materials. Also, the surface coverage of each functionalised fibres was estimated from cyclic voltammetry, while in the case of the *p*-nitro functionalisation it was directly calculated making use of the redox properties of this functional group. The resulting modified CNTFs feature multiple possibilities to farther modified

Table 1 Surface coverage Γ of functionalisation on the CNTFs after the reaction with different diazonium salts

Sample	$\Gamma_{reaction}{}^a$ (mol cm^{-2})	$\Gamma_{CNTF}{}^b$ (mol cm^{-2})
CNTF1	7.27 ± 1.06 × 10^{-9}	—
CNTF2	34.5 ± 3.21 × 10^{-9}	—
CNTF3	2.91 ± 0.74 × 10^{-9}	2.37 ± 0.68 × 10^{-9}
CNTF4	4.08 ± 0.31 × 10^{-9}	—

^{a} $\Gamma_{reaction}$ was calculated from the charge Q used for the reduction of the diazonium salt. ^{b} Γ_{CNTF} was obtained making use of a redox moiety grafted to the CNTF3 (*vide-infra*).

the CNTF surface through further reactions on the introduced moieties. Indeed, we foresee applying this approach to such modified materials in the sensing and biomedical fields, in which the introduction of anchor points, such as amines or carboxylic acids, are mandatory to anchor active molecules or receptors on the fibre surface through fast, non-damaging, and controllable procedures are highly desirable.

Author contributions

M. Pasquali, M. Prato, A. B., and A. C. conceptualised the project and designed the experiments. A. D.-A., N. C., S. Y., D. M., S. P., S. W., L. T., O. D., and A. C. performed the experiments and analysed the data. A. D.-A, A. C., and D. M. wrote the original draft. M. Pasquali, M. Prato, A. B., and A. C. supervised the works and acquired funding. All the authors participated to the writing, reviewing, and editing of the manuscript. All authors discussed the results and contributed to the manuscript.

Conflicts of interest

M. Pasquali has a financial interest in DexMat, Inc., which commercialises CNTFs similar to the ones used in this article.

Acknowledgements

References

1 A. Hirsch, The era of carbon allotropes, *Nat. Mater.*, 2010, **9**, 868–871.

2 N. Behabtu, C. C. Young, D. E. Tsentalovich, O. Kleinerman, X. Wang, A. W. K. Ma, E. A. Bengio, R. F. Ter Waarbeek, J. J. De Jong, R. E. Hoogerwerf, S. B. Fairchild, J. B. Ferguson, B. Maruyama, J. Kono, Y. Talmon, Y. Cohen, M. J. Otto and M. Pasquali, Strong, light, multifunctional fibers of carbon nanotubes with ultrahigh conductivity, *Science*, 2013, **339**, 182–186.

3 J. C. Stallard, W. Tan, F. R. Smail, T. S. Gspann, A. M. Boies and N. A. Fleck, The mechanical and electrical properties of direct-spun carbon nanotube mats, *Extreme Mech. Lett.*, 2018, **21**, 65–75.

4 L. W. Taylor, O. S. Dewey, R. J. Headrick, N. Komatsu, N. M. Peraca, G. Wehmeyer, J. Kono and M. Pasquali, Improved properties, increased production, and the path to broad adoption of carbon nanotube fibers, *Carbon*, 2021, **171**, 689–694.

5 M. Barrejón, R. Rauti, L. Ballerini and M. Prato, Chemically cross-linked carbon nanotube films engineered to control neuronal signaling, *ACS Nano*, 2019, **13**, 8879–8889.

6 V. Sgobba and D. M. Guldi, 2009 Renewable Energy issue energy research, *Chem. Soc. Rev.*, 2009, **38**, 165–184.

7 W. Hoenlein, F. Kreupl, G. S. Duesberg, A. P. Graham, M. Liebau, R. Seidel and E. Unger, Carbon nanotubes for microelectronics: status and future prospects, *Mater. Sci. Eng., C*, 2003, **23**, 663–669.

8 X. Gui, J. Wei, K. Wang, A. Cao, H. Zhu, Y. Jia, Q. Shu and D. Wu, Carbon nanotube sponges, *Adv. Mater.*, 2010, **22**, 617–621.

9 A. Dominguez-Alfaro, N. Alegret, B. Arnaiz, J. M. González-Domínguez, A. Martin-Pacheco, U. Cossío, L. Porcarelli, S. Bosi, E. Vázquez, D. Mecerreyes and M. Prato, Tailored Methodology Based on Vapor Phase Polymerization to Manufacture PEDOT/CNT Scaffolds for Tissue Engineering, *ACS Biomater. Sci. Eng.*, 2020, **6**, 1269–1278.

10 N. Alegret, A. Dominguez-Alfaro, J. M. González-Domínguez, B. Arnaiz, U. Cossío, S. Bosi, E. Vázquez, P. Ramos-Cabrer, D. Mecerreyes and M. Prato, Three-Dimensional Conductive Scaffolds as Neural Prostheses Based on Carbon Nanotubes and Polypyrrole, *ACS Appl. Mater. Interfaces*, 2018, **10**, 43904–43914.

11 D. E. Tsentalovich, R. J. Headrick, F. Mirri, J. Hao, N. Behabtu, C. C. Young and M. Pasquali, Influence of Carbon Nanotube Characteristics on Macroscopic Fiber Properties, *ACS Appl. Mater. Interfaces*, 2017, **9**, 36189–36198.

12 B. Vigolo, A. Penicaud, C. Coulon, C. Sauder, R. Pailler, C. Journet, P. Bernier and P. Poulin, Macroscopic fibers and ribbons of oriented carbon nanotubes, *Science*, 2000, **290**, 1331–1334.

13 Y. L. Li, I. A. Kinloch and A. H. Windle, Direct Spinning of Carbon Nanotube Fibers from Chemical Vapor Deposition Synthesis, *Science*, 2004, **304**, 276–278.

14 M. Zhang, K. R. Atkinson and R. H. Baughman, Multifunctional carbon nanotube yarns by downsizing an ancient technology, *Science*, 2004, **306**, 1358–1361.

15 V. A. Davis, A. N. G. Parra-Vasquez, M. J. Green, P. K. Rai, N. Behabtu, V. Prieto, R. D. Booker, J. Schmidt, E. Kesselman, W. Zhou, H. Fan, W. W. Adams, R. H. Hauge, J. E. Fischer, Y. Cohen, Y. Talmon, R. E. Smalley and M. Pasquali, True solutions of single-walled carbon nanotubes for assembly into macroscopic materials, *Nat. Nanotechnol.*, 2009, **4**, 830–834.

16 L. M. Ericson, H. Fan, H. Peng, V. A. Davis, W. Zhou, J. Sulpizio, Y. Wang, R. Booker, J. Vavro, C. Guthy, A. N. G. Parra-vasquez, M. J. Kim, S. Ramesh, R. K. Saini, C. Kittrell, G. Lavin, H. Schmidt, W. W. Adams, W. E. Billups, M. Pasquali, W. Hwang, R. H. Hauge, J. E. Fischer and R. E. Smalley, Macroscopic, Neat, Single-Walled Carbon Nanotube Fibers, *Science*, 2004, **305**, 1447–1451.

17 V. Jamali, F. Niroui, L. W. Taylor, O. S. Dewey, B. A. Koscher, M. Pasquali and A. P. Alivisatos, Perovskite-Carbon Nanotube Light-Emitting Fibers, *Nano Lett.*, 2020, **20**, 3178–3184.

18 M. D. Mccauley, F. Vitale, J. S. Yan, C. C. Young, B. Greet, M. Orecchioni, S. Perike, A. Elgalad, J. A. Coco, M. John, D. A. Taylor, L. C. Sampaio, L. G. Delogu, M. Razavi and M. Pasquali, In Vivo Restoration of Myocardial Conduction With Carbon Nanotube Fibers, *Circ.: Arrhythmia Electrophysiol.*, 2019, **12**, 1–15.

19 C. Liu, Q. Zhang, F. Stellacci, N. Marzari, L. Zheng and Z. Zhan, Carbene-functionalized single-walled carbon nanotubes and their electrical properties, *Small*, 2011, **7**, 1257–1263.

20 M. S. Strano, C. A. Dyke, M. L. Usrey, P. W. Barone, M. J. Allen, H. Shan, C. Kittrell, R. H. Hauge, J. M. Tour and R. E. Smalley, Electronic structure control of single-waited carbon nanotube functionalization, *Science*, 2003, **301**, 1519–1522.

21 G. Reina, J. M. González-Domínguez, A. Criado, E. Vázquez, A. Bianco and M. Prato, Promises, facts and challenges for graphene in biomedical applications, *Chem. Soc. Rev.*, 2017, **46**, 4400–4416.

22 D. Tasis, N. Tagmatarchis, A. Bianco and M. Prato, Chemistry of Carbon Nanotubes, *Nanostruct. Mater.*, 2006, **106**, 1105–1136.

23 N. Karousis and N. Tagmatarchis, Current Progress on the Chemical Modification of Carbon Nanotubes, *Chem. Rev.*, 2010, **110**, 5366–5397.

24 Z. Q. Zhang, B. Liu, Y. L. Chen, H. Jiang, K. C. Hwang and Y. Huang, Mechanical properties of functionalized carbon nanotubes, *Nanotechnology*, 2008, **19**, 395702.

25 A. Garg and S. B. Sinnott, Effect of chemical functionalization on the mechanical properties of carbon nanotubes, *Chem. Phys. Lett.*, 1998, **295**, 273–278.

26 J. M. González-Domínguez, A. Santidrián, A. Criado, C. Hadad, M. Kalbáč and T. Da Ros, Multipurpose Nature of Rapid Covalent Functionalization on Carbon Nanotubes, *Chem. – Eur. J.*, 2015, **21**, 18631–18641.

27 T. H. Phan, H. Van Gorp, Z. Li, T. M. Trung Huynh, Y. Fujita, L. Verstraete, S. Eyley, W. Thielemans, H. Uji-I, B. E. Hirsch, S. F. L. Mertens, J. Greenwood, O. Ivasenko and S. De Feyter, Graphite and Graphene Fairy Circles: A Bottom-Up Approach for the Formation of Nanocorrals, *ACS Nano*, 2019, **13**, 5559–5571.

28 E. Er, H.-L. Hou, A. Criado, J. Langer, M. Möller, N. Erk, L. M. Liz-Marzán and M. Prato, High-Yield Preparation of Exfoliated 1T-MoS 2 with SERS Activity, *Chem. Mater.*, 2019, **31**, 5725–5734.

29 C. Saby, B. Ortiz, G. Y. Champagne and D. Bélanger, Electrochemical modification of glassy carbon electrode using aromatic diazonium salts. 1. Blocking effect of 4-nitrophenyl and 4-carboxyphenyl groups, *Langmuir*, 1997, **13**, 6805–6813.

30 M. Delamar, G. Désarmot, O. Fagebaume, R. Hitmi, J. Pinson and J. M. Savéant, Modification of carbon fiber surfaces by electrochemical reduction of aryl diazonium salts: Application to carbon epoxy composites, *Carbon*, 1997, **35**, 801–807.

31 D. Belangera and J. Pinsonb, Electrografting : a powerful method for surface modification, *Chem. Soc. Rev.*, 2011, **40**, 3995–4048.

32 C. Cao, Y. Zhang, C. Jiang, M. Qi and G. Liu, Advances on Aryldiazonium Salt Chemistry Based Interfacial Fabrication for Sensing Applications, *ACS Appl. Mater. Interfaces*, 2017, **9**, 5031–5049.

33 J. M. Chrétien, M. A. Ghanem, P. N. Bartlett and J. D. Kilburn, Covalent tethering of organic functionality to the surface of glassy carbon electrodes by using electro-chemical and solid-phase synthesis, *Chem. – Eur. J.*, 2008, **14**, 2548–2556.

34 H. H. Gommans, J. W. Alldredge, H. Tashiro, J. Park, J. Magnuson and A. G. Rinzler, Fibers of aligned single-walled carbon nanotubes: Polarized Raman spectroscopy, *J. Appl. Phys.*, 2000, **88**, 2509–2514.

35 R. J. Headrick, D. E. Tsentalovich, J. Berdegué, E. A. Bengio, L. Liberman, O. Kleinerman, M. S. Lucas, Y. Talmon and M. Pasquali, Structure–Property Relations in Carbon Nanotube Fibers by Downscaling Solution Processing, *Adv. Mater.*, 2018, **30**, 1–8.

36 C. Cougnon, N. H. Nguyen, S. Dabos-Seignon, J. Mauzeroll and D. Bélanger, Carbon surface derivatization by electrochemical reduction of a diazonium salt in situ produced from the nitro precursor, *J. Electroanal. Chem.*, 2011, **661**, 13–19.

37 A. Adenier, M. M. Chehimi, I. Gallardo and J. Pinson, Electrochemical Oxidation of Aliphatic Amines and Their Attachment to Carbon and Metal Surfaces, *Langmuir*, 2004, **20**, 8243–8253.

38 V. Georgakilas, N. Tagmatarchis, D. Pantarotto, A. Bianco, J. P. Briand and M. Prato, Amino acid functionalisation of water soluble carbon nanotubes, *Chem. Commun.*, 2002, 3050–3051.

39 C. Fantini, M. L. Usrey and M. S. Strano, Investigation of electronic and vibrational properties of single-walled carbon nanotubes functionalized with diazonium salts, *J. Phys. Chem. C*, 2007, **111**, 17941–17946.

40 D. Ullien, P. C. Thüne, W. F. Jager, E. J. R. Sudhölter and L. C. P. M. de Smet, Controlled amino-functionalization by electrochemical reduction of bromo and nitro azobenzene layers bound to Si(111) surfaces, *Phys. Chem. Chem. Phys.*, 2014, **16**, 19258–19265.

41 K. Kishi, H. Takata and S. Kohnushi, Nitrobenzene adsorption on clean and NaCl-covered Cu(100), Ni/Cu(100), Ag/Cu (100) and Na/Cu(100) surfaces studied by XPS and XAES, *J. Electron Spectrosc. Relat. Phenom.*, 1992, **61**, 83–101.

42 R. H. Baughman, A. A. Zakhidov and W. A. De Heer, Carbon nanotubes - The route toward applications, *Science*, 2002, **297**, 787–792.

43 S. Porada, R. Zhao, A. Van Der Wal, V. Presser and P. M. Biesheuvel, Review on the science and technology of water desalination by capacitive deionization, *Prog. Mater. Sci.*, 2013, **58**, 1388–1442.

44 G. G. Wildgoose, C. E. Banks, H. C. Leventis and R. G. Compton, Chemically modified carbon nanotubes for use in electroanalysis, *Microchim. Acta*, 2006, **152**, 187–214.

45 J. Shen, A. Liu, Y. Tu, G. Foo, C. Yeo, M. B. Chan-Park, R. Jiang and Y. Chen, How carboxylic groups improve the performance of single-walled carbon nanotube electrochemical capacitors?, *Energy Environ. Sci.*, 2011, **4**, 4220–4229.

46 J. R. Miller, R. A. Outlaw and B. C. Holloway, Graphene double-layer capacitor with ac line-filtering performance, *Science*, 2010, **329**, 1637–1639.

47 J. Joseph, A. Paravannoor, S. V. Nair, Z. J. Han, K. Ostrikov and A. Balakrishnan, Supercapacitors based on camphor-derived meso/macroporous carbon sponge electrodes with ultrafast frequency response for ac line-filtering, *J. Mater. Chem. A*, 2015, **3**, 14105–14108.

48 J. Greenwood, T. H. Phan, Y. Fujita, Z. Li, O. Ivasenko, W. Vanderlinden, H. Van Gorp, W. Frederickx, G. Lu, K. Tahara, Y. Tobe, H. Uji-I, S. F. L. Mertens and S. De Feyter, Covalent modification of graphene and graphite using diazonium chemistry: Tunable grafting and nanomanipulation, *ACS Nano*, 2015, **9**, 5520–5535.

49 S. Sarkar, E. Bekyarova, S. Niyogi and R. C. Haddon, Diels-Alder chemistry of graphite and graphene: Graphene as diene and dienophile, *J. Am. Chem. Soc.*, 2011, **133**, 3324–3327.

50 E. Bekyarova, M. E. Itkis, P. Ramesh, C. Berger, M. Sprinkle, W. a de Heer and R. C. Haddon, Chemical modification of epitaxial graphene: spontaneous grafting of aryl groups., *J. Am. Chem. Soc.*, 2009, **131**, 1336–1337.

51 M. Z. Hossain, M. a Walsh and M. C. Hersam, Scanning tunneling microscopy, spectroscopy, and nanolithography of epitaxial graphene chemically modified with aryl moieties, *J. Am. Chem. Soc.*, 2010, **132**, 15399–15403.

52 A. Cyr, P. Huot, J. F. Marcoux, G. Belot, E. Laviron and J. Lessard, The electrochemical reduction of nitrobenzene and azoxybenzene in neutral and basic aqueous methanolic solutions at polycrystalline copper and nickel electrodes, *Electrochim. Acta*, 1989, **34**, 439–445.

53 W. Richard, D. Evrard and P. Gros, New insight into 4-nitrobenzene diazonium reduction process: Evidence for a grafting step distinct from NO2 electrochemical reactivity, *J. Electroanal. Chem.*, 2012, **685**, 109–115.

54 Z. Nazemi, E. Shams and M. K. Amini, Covalent modification of glassy carbon electrode by Nile blue: Preparation, electrochemistry and electrocatalysis, *Electrochim. Acta*, 2010, **55**, 7246–7253.

55 P. A. Brooksby and A. J. Downard, Multilayer nitroazobenzene films covalently attached to carbon. An AFM and electrochemical study, *J. Phys. Chem. B*, 2005, **109**, 8791–8798.